Steel and Composite Structures, *Vol. 20, No. 1 (2016) 205-225*
DOI: http://dx.doi.org/10.12989/scs.2016.20.1.205

Deflection and vibration analysis of higher-order shear deformable compositionally graded porous plate

Farzad Ebrahimi* and Sajjad Habibi

Mechanical Engineering Department, *Faculty of Engineering*, *Imam Khomeini International University*, *Qazvin*, *Iran P.O.B. 16818-34149*

(*Received March 30, 2015, Revised July 10, 2015, Accepted August 23, 2015*)

Abstract. In this study the finite element method is utilized to predict the deflection and vibration characteristics of rectangular plates made of saturated porous functionally graded materials (PFGM) within the framework of the third order shear deformation plate theory. Material properties of PFGM plate are supposed to vary continuously along the thickness direction according to the power-law form and the porous plate is assumed of the form where pores are saturated with fluid. Various edge conditions of the plate are analyzed. The governing equations of motion are derived through energy method, using calculus of variations while the finite element model is derived based on the constitutive equation of the porous material. According to the numerical results, it is revealed that the proposed modeling and finite element approach can provide accurate deflection and frequency results of the PFGM plates as compared to the previously published results in literature. The detailed mathematical derivations are presented and numerical investigations are performed while the emphasis is placed on investigating the effect of the several parameters such as porosity volume fraction, material distribution profile, mode number and boundary conditions on the natural frequencies and deflection of the PFGM plates in detail. It is explicitly shown that the deflection and vibration behaviour of porous FGM plates are significantly influenced by these effects. Numerical results are presented to serve as benchmarks for future analyses of FGM plates with porosity phases.

Keywords: porous materials; finite element analysis; higher order shear deformation plate theory; vibration; deflection; functionally graded material

1. Introduction

Porous materials which frequently found in nature such as wood, stone, and layers of dust are composed of two elements: One element is a solid (body), and the other element is either liquid or gas. During the last several years, porous material structures such as beams, plates, and shells have been used widely in structural design problems. Biot is the pioneer to develop the field of poroelasticity interactions (Biot 1941). He introduced the following bulk dynamic and kinematic variables (in the current notation); the total stress tensor σ_{ij}, the fluid pressure p, the solid strain tensor ε_{ij}, and the variation of fluid volume content ζ. In his model, the deformable porous medium is considered as a continuum consisting of a solid phase and fluid phase. Latter, Biot reformulated his theory using the concept of partial stresses (Biot 1955). The vibrations of porous structures are

*Corresponding author, Dr. Farzad Ebrahimi, E-mail: febrahimy@eng.ikiu.ac.ir

http://www.techno-press.org/?journal=scs&subpage=8 ISSN: 1229-9367 (Print), 1598-6233 (Online)

important in problems of sound absorption and in the aeronautical industry. The vibration of porous beams and plates has been scarcely studied analytically to date. Significant result has been given by Theodorakopoulos and Beskos (1994), who have extended the classical theory of thin rectangular plates to porous materials including Biot's stress-strain relations in porous media (Biot 1956). They have established two coupled governing equations and have given the solutions for a simply supported plate by extending Navier's algebraic solution to the porous case. Making an additional assumption about the fluid-solid relative displacement and using an alternate form of Biot's relations, Leclaire *et al*. (2001) have proposed two equations of equilibrium, which are valid in applications where the plate is thinner than any acoustic wavelength. They also presented the vibrational behaviour of a rectangular porous plate described by two coupled equations involving the time and space derivatives of the deflection and of the relative fluid-solid motion.

In an effort to develop the super heat resistant materials, Japanese materials scientists proposed the concept of functionally graded materials (FGM) (Ebrahimi and Rastgoo 2008a, b). FGMs are composite materials with inhomogeneous micromechanical structure. These materials, which are microscopically heterogeneous and are typically made from isotropic components, such as metals and ceramics, were initially designed as thermal barrier materials for aerospace structures and fusion reactors (Ebrahimi 2013). Continuous changes in the composition, microstructure, porosity, etc. of these materials results in gradients in such properties as mechanical strength and thermal conductivity.

Presenting novel properties, FGMs have also attracted intensive research interests, which were mainly focused on their static, dynamic and vibration characteristics of FG structures (Ebrahimi *et al*. 2009a, b). Among them, Reddy (2000) used third-order shear deformation theory (TSDT) and finite element method to study the static and dynamic analysis of functionally graded. Ferreira *et al*. (2006) used the first and the third-order shear deformation theories and Mori–Tanaka homogenization method and the global collocation method with multi-quadratic radial basis functions to obtain the free vibration of FG plates. Vel and Batra (2007) presented a three dimensional exact solution for the free and forced vibrations of simply supported rectangular plates. Batra and Jin (2005) used first-order shear deformation theory (FSDT) and finite element method to study the free vibrations of functionally graded anisotropic plates under different boundary conditions. Zenkour (2009) presented a sinusoidal shear deformation theory for FGM plates on elastic foundations. Brischetto (2013) used exact elasticity solution for study natural frequencies of functionally graded simply-supported structures.

Ebrahimi and Rastgoo (2011) presented a theoretical model for geometrically nonlinear vibration analysis of thermo-piezoelectrically actuated circular plates made of FGM based on Kirchhoff's–Love hypothesis with von-Karman type geometrical large nonlinear deformations. Reddy and Cheng (2003) obtained the frequencies of functionally graded rectangular plates by using a three-dimensional asymptotic approach. Thus, there is a lot of studies which have analyzed vibrational and stability behaviors of FG beams and plates but the majority of these studies considered FGM in their analysis because of their high mechanical–thermal resistant and FGM plates with porosity are less mentioned.

Because of existence of technical problem in manufacturing of FGM, porosity or micro voids occurring inside FGM, thus it is necessary to consider the effect of porosity on static and dynamic's behavior of porous FGM (PFGM) structures. In the area of vibration analysis of FG porous structures, Recently, Ebrahimi and Mokhtari (2014) presented transverse vibration analysis of rotating functionally graded beam with porosity based on Timoshenko beam theory. The differential transform method was used to solve the equations of motion subjected to different

boundary conditions. They showed that increasing the volume fraction of porosity leads to a slight increase in the fundamental frequencies. Additionally, Wattanasakulpong and Chaikittiratana (2015) investigated flexural vibration of imperfect FGM beams based on Timoshenko beam theory by using Chebyshev collocation method (CCM). Moreover Khorshidvand *et al*. (2014) studied the stability of porous circular plate with sensor actuator patches. Further Jabbari *et al*. (2013a, 2014ab) studied the mechanical buckling of porous circular plate based on classical plate theory. They investigated the effect of porosity and pore fluid properties on critical mechanical buckling load. They also investigated the thermal buckling analysis of porous circular plate with piezoelectric actuators based on FSDT (Jabbari *et al*. 2014b) and the thermal buckling behaviour of FG circular plate based on higher order shear deformation plate theory (HSDPT) (Jabbari *et al*. 2013b).

It is worth mentioning that all aforementioned studies focused on the buckling and stability behaviour of porous FG plates and to the authors' best knowledge, no research dealing with the deflection and vibration characteristics of the rectangular FG plates made of porous materials has been reported in literature.

Also engineering problems deal with two main concepts: the modeling of the structures and the procedure of solution. These problems are often described by partial differential equations. However, analytical solutions of partial differential equations are obtained only a few special cases. Consequently, the solution of the mathematical model is usually obtained by numerical methods. A main principle of the numerical methods is the reduction of a differential equation to an approximation in terms of algebraic equations. This reduction replaces a continuous differential equation, whose solution space is generally infinite dimensional, with a finite set of algebraic equations whose solution space is finite dimensional (Civalek 2013). Large number of useful methods have been developed to obtain solutions for many practical problems.

Typical successful numerical methods include the spline finite strip, the Galerkin, the least squares technique and Rayleigh-Ritz methods. In particular differential quadrature (DQ) methods have many successful applications in the vibration analysis. The DQ is based on the idea that the partial derivative of a function with respect to a spatial variable at a given discrete point can be expressed as a weighted linear sum of the function values at all the discrete points in the computational domain (Ng *et al*. 2004). Of another these methods is Discrete singular convolution (DSC). This method is a relatively new numerical discretization technique for approximation of derivatives (Civalek 2009, 2013). After proposed, the method of DSC has been increasingly applied to solve differential equations in many engineering and sciences problems.

In the past 10 years, the meshless methods for numerical analysis of partial differential equations have become quite popular. They can be subdivided in accordance with the definition of the shape functions. Important type of meshless methods are the smoothed particle hydrodynamics, diffuse element method, element-free Galerkin method, reproducing kernel particle methods, meshless local Petrov-Galerkin method (Civalek 2008).

Finite element methods often divide the domain of interest into a number of smaller sub-domains, and approximate the solution by using local, piecewise continuous shape functions. Finite element models can be developed based on the classical plate theory (CPT), FSDT and HSDT. The CPT known as Kirchhoff plate theory is the simplest one and is applicable to thin plate only. The FSDT, known as Mindlin plate theory, accounts for the shear deformation effects by way of linear variation of in-plane displacements through the thickness. Since the FSDT violates the equilibrium conditions on the top and bottom surfaces of the plate, a shear correction factor is required to compensate for the error due to a constant shear strain assumption through the thickness. Although the FSDT provides a sufficiently accurate description of response for thin to

moderately thick laminates, it is not convenient for use due to the difficulty in calculating correct value of the shear correction factor. To avoid the use of shear correction factor and have a better prediction of response of laminated plates, many HSDTs have been developed (Thai and Choi 2014).

Thus in this paper, deflection and vibration characteristics of functionally graded rectangular plate made of porous materials are investigated by presenting a finite element formulation within the framework of the higher order shear deformation plate theory. The material properties of the FG plate are assumed to be graded in the thickness direction according to the power-law distribution in terms of the volume fractions of the constituents while the porous plate is assumed of the from where pores are saturated with fluid. The method of calculus of variations are utilized in order to stablish the governing equations of the problem and the numerical examples are provided and simulation results are discussed. Numerical results for PFGM plates with a mixture of metal and ceramic are presented in dimensionless forms. The good agreement between the results of this paper and those available in literature validated the presented approach. A parametric study is also undertaken to highlight the effects of several parameters such as porosity volume fraction, material distribution profile, mode number and boundary conditions on the natural frequencies and deflection of the PFGM plates.

2. Mathematical formulation

Consider a rectangular plate made of porous material with co-ordinates x and y along the in-plane directions and z along the thickness direction as shown in Fig. 1. The coordinate axis is assumed to lie on the middle plane of the plate with z showing the variable across the plate cross section. The functional relationship between E and z for porous plate is assumed as (Magnucka-Blandzi 2008).

$$\begin{gathered} G(z) = G_0\left[1 - e_1\cos\left(\left(\frac{\pi}{2h}\right)\left(z+\frac{h}{2}\right)\right)\right] \\ E(z) = E_0\left[1 - e_1\cos\left(\left(\frac{\pi}{2h}\right)\left(z+\frac{h}{2}\right)\right)\right] \\ \rho(z) = \rho_0\left[1 - e_m\cos\left(\left(\frac{\pi}{2h}\right)\left(z+\frac{h}{2}\right)\right)\right] \\ e_1 = 1 - \frac{G_0}{G_1} = 1 - \frac{E_0}{E_1} \\ e_m = 1 - \sqrt{1-e_1} \end{gathered} \tag{1}$$

where e_1 is the coefficient of plate porosity $0 < e_1 < 1$, E_1 and E_0 Young's modulus of elasticity at $z = -h/2$ and $z = h/2$, respectively, and G_0 and G_1 are the shear modulus at $z = -h/2$ and $z = h/2$, respectively. The relationship between the modulus of elasticity and shear modulus for $j = 0$

and 1 is $E_j = 2G_j\ (1 + v)$ and v is Poisson's ratio, which is assumed to be constant across the plate thickness. Mechanical properties of the porous material vary across the thickness of the plate, ($G_1 \geq G_0$).

2.1 Displacement field and strain

The displacement field is assumed according to the HSDPT

$$u = u_0 + z\phi_x - c_1 z^3 \left(\phi_x + \frac{\partial w_0}{\partial \mathrm{x}}\right);$$

$$v = v_0 + z\phi_y - c_1 z^3 \left(\phi_y + \frac{\partial w_0}{\partial \mathrm{y}}\right); \tag{2}$$

$$w = w_0$$

where u_0, v_0, and w_0 denote the displacements at the mid-plane of the plate in the x; y, and z directions and ϕ_x and ϕ_y represent the transverse normal rotations about the y and x axes, respectively and $c_1 = 4/3h^2$. The strain–displacement relations, based on von Karman's large deformation assumption using HSDPT, are (Reddy 2004)

$$\begin{Bmatrix}\varepsilon_{xx}\\ \varepsilon_{yy}\\ \gamma_{xy}\end{Bmatrix} = \varepsilon_0 + z\varepsilon_1 + z^3\varepsilon_3\ , \qquad \begin{Bmatrix}\gamma_{yz}\\ \gamma_{xz}\end{Bmatrix} = \gamma_0 + z^2\gamma_2 \tag{3a}$$

where

$$\varepsilon_0 = \begin{Bmatrix} \dfrac{\partial u_0}{\partial \mathrm{x}} \\ \dfrac{\partial v_0}{\partial \mathrm{y}} \\ \dfrac{\partial u_0}{\partial \mathrm{y}} + \dfrac{\partial v_0}{\partial \mathrm{x}} \end{Bmatrix}, \qquad \varepsilon_1 = \begin{Bmatrix} \dfrac{\partial \phi_x}{\partial \mathrm{x}} \\ \dfrac{\partial \phi_y}{\partial \mathrm{y}} \\ \dfrac{\partial \phi_x}{\partial \mathrm{y}} + \dfrac{\partial \phi_y}{\partial \mathrm{x}} \end{Bmatrix}$$

$$\varepsilon_3 = -c_1 \begin{Bmatrix} \dfrac{\partial \phi_x}{\partial \mathrm{x}} \\ \dfrac{\partial \phi_y}{\partial \mathrm{y}} \\ \dfrac{\partial \phi_x}{\partial \mathrm{y}} + \dfrac{\partial \phi_y}{\partial \mathrm{x}} \end{Bmatrix}, \qquad \gamma_0 = \begin{Bmatrix} \dfrac{\partial w_0}{\partial x} + \phi_x \\ \dfrac{\partial w_0}{\partial y} + \phi_y \end{Bmatrix} \tag{3b}$$

$$\gamma_0 = -c_2 \begin{Bmatrix} \dfrac{\partial w_0}{\partial x} + \phi_x \\ \dfrac{\partial w_0}{\partial y} + \phi_y \end{Bmatrix}$$

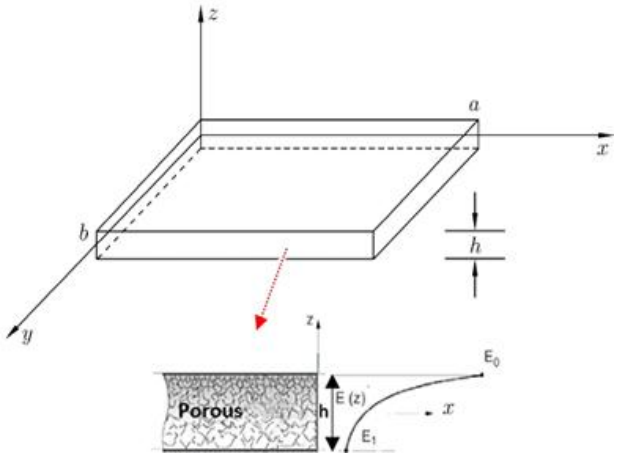

Fig. 1 Geometry of a FG porous rectangular plate and variation of modulus through the thickness

In the above relations, ε_{xx}, ε_{yy} and γ_{xy} denote in-plane strains. Also, γ_{yz} and γ_{xz} are transverse shear strains and $c_2 = 3c_1$.

2.2 Constitutive relations

In this study, constant transverse normal displacement (zero transverse normal strain) in displacement field is assumed in Eq. (2). In order to avoid Poisson locking, zero transverse normal stress (σ_z = 0) must be imposed in constitutive equations (Carrera and Brischetto 2008). By setting σ_z = 0 in the constitutive relations and solving it for ε_z and then substituting the result in the remaining equations, reduced constitutive relations are obtained. The linear poroelasticity theory of Biot has two features namely, an increase of pore pressure induces a dilation of pore and compression of the pore causes a rise of pore pressure (Biot 1964). Thus the stress-strain law for the poroelasticity is given by (Ghassemi and Zhang 2004)

$$\sigma_{ij} = 2G\epsilon_{ij} + \frac{2G\nu_u}{1-2\nu_u}\epsilon\delta_{ij} - p\alpha\delta_{ij}$$

$$p = M(\zeta - \alpha\epsilon)$$

$$M = \frac{2G(\nu_u - \nu)}{\alpha^2(1-2\nu_u)(1-2\nu)} \tag{4}$$

$$\nu_u = \frac{\nu + \frac{\alpha B(1-2\nu)}{3}}{1 - \frac{\alpha B(1-2\nu)}{3}}$$

Here P is pore fluid pressure, M is Biot's modulus, G is shear modulus, ν_u is undrained Poisson's ratio $\nu < \nu_u < 0/5$, α is the Biot coefficient of effective stress $0 < \alpha < 1$, ϵ is the volumetric strain, and ζ is variation of fluid volume content, B is Skempton coefficient, the pore

fluid properties is introduced by the Skempton coefficient.

Biot's coefficients of interest in this study are and *M* and are given by (Biot and Willis 1957)

$$\alpha = \phi\left(1+\frac{Q}{R}\right), \qquad M=\frac{R}{\phi^2} \tag{0}$$

where the elastic coefficients *Q* and *R* can be written as

$$Q=\frac{(1-c)\phi_s\phi}{\frac{(1-c)\phi_s}{K_s}+\frac{\phi}{K_f}}, \qquad R=\frac{\phi^2}{\frac{(1-c)\phi_s}{K_s}+\frac{\phi}{K_f}} \tag{0}$$

In which

$$c=\frac{K}{\phi_s K_s} \qquad \text{and} \qquad \phi_s = 1-\phi \tag{0}$$

In these expressions, K_f, K_s and K are, respectively, the bulk moduli of the solid constituting the frame, of the fluid and of the frame at constant fluid pressure. The coefficient *c* can be seen as a coefficient characterizing the consolidation state of the heterogeneous material. Since *K* is less than the Hashin-Strikman upper bound $\phi_s K_s$ (Hashin and Strikman 1963), *c* is between 0 (non-consolidated materials) and 1 (consolidated materials). The following relation is further obtained

$$\alpha = 1-c\phi_s \tag{0}$$

And the bounds for α are ϕ (consolidated materials) and 1 (non-consolidated materials). It is interesting to note the similarity for $c = 0$ between the expression for *Q* and *R* and the Hashin-Strikman lower bound. Biot's elastic coefficients can be determined from hydrostatic experiments (Fatt 1959). Since the fluid is air, the approximation $K_f \ll K_f$, *K* can be made. The materials are fairly rigid and so we shall also consider that $c = 1$ and $\alpha = \phi$ in the numerical computation. As a result, the coefficients of interest are approximated by

$$Q \cong 0, \qquad R \cong \phi K_f, \qquad M=\frac{K_f}{\phi} \tag{0}$$

The two dimensional stress–strain law for plane-stress condition and when ($\zeta = 0$) is given by

$$\begin{Bmatrix}\sigma_{xx}\\ \sigma_{yy}\\ \sigma_{xy}\end{Bmatrix} = [Q]\begin{Bmatrix}\epsilon_{xx}\\ \epsilon_{yy}\\ \epsilon_{xy}\end{Bmatrix}, \qquad \begin{Bmatrix}\tau_{yz}\\ \tau_{xz}\end{Bmatrix} = [Q_s]\begin{Bmatrix}\gamma_{yz}\\ \gamma_{xz}\end{Bmatrix} \tag{5}$$

$$Q=G(z)\begin{bmatrix}P_1 & P_2 & 0\\ P_2 & P_1 & 0\\ 0 & 0 & 1\end{bmatrix}, \qquad Q_s = k_s G(z)\begin{bmatrix}1 & 0\\ 0 & 1\end{bmatrix} \tag{6}$$

$$\begin{aligned} P_1 &= \left(\frac{2}{1-{\nu_u}^2}\right)\left[1+\nu_u+\frac{(\nu_u-\nu)(1+\nu_u)}{(1-2\nu)}\left(1-\frac{C_2}{C_1}\right)\right]\\ P_2 &= \left(\frac{2}{1-{\nu_u}^2}\right)\left[(1+\nu_u)\nu_u+\frac{(\nu_u-\nu)(1+\nu_u)}{(1-2\nu)}\left(1-\frac{C_2}{C_1}\right)\right] \end{aligned} \tag{7}$$

$$C_1 = 2\left[1 + \frac{\nu_u}{(1-2\nu_u)} + \frac{(\nu_u - \nu)}{(1-2\nu_u)(1-2\nu)}\right] G(z)$$
$$C_2 = C_1 - 2G(z) \tag{7}$$

3. Finite element model

The potential energy of an FG porous plate is given as follows

$$\int_0^T (\delta U - \delta W) dt = 0 \tag{8}$$

$$\begin{aligned} \delta U &= \int_{\Omega_0} \int_{-\frac{h}{2}}^{\frac{h}{2}} \delta\epsilon^T \sigma . dz d\Omega_0 \\ &= \int_{\Omega_0} \{ \int_{-\frac{h}{2}}^{\frac{h}{2}} [\sigma_x \, \delta\epsilon_x + \sigma_y \delta\epsilon_y + \tau_{xy} \delta\gamma_{xy} + \tau_{xz} \delta\gamma_{xz} + \tau_{yz} \delta\gamma_{yz}] dz \} d\Omega_0 \end{aligned} \tag{9a}$$

$$\begin{aligned} \delta W = &- \int_{\Omega_0} \int_{-\frac{h}{2}}^{\frac{h}{2}} \rho_0 (\ddot{u}\delta u + \ddot{v}\delta v + \ddot{w}\delta w) dz d\Omega_0 \\ &+ \int_{\Gamma_\sigma} \int_{-\frac{h}{2}}^{\frac{h}{2}} [\hat{\sigma}_n (\delta u_n + z\delta\psi_n) + \hat{\sigma}_{ns} (\delta u_s + z\delta\psi_s) + \hat{\sigma}_{nz} \delta w_0] dz ds \end{aligned} \tag{9b}$$

where Ω_0 and Γ_σ represent respectively area of the reference plane and the boundary of the plate and the subscripts, n and s denote directions normal and tangent to the boundary, respectively. And

$$\begin{cases} \psi_n = \psi_x n_x + \psi_y n_y \, , \psi_s = \psi_y n_x - \psi_x n_y \\ u_n = u_0 n_x + v_0 n_y \, , \psi_s = v_0 n_x - u_0 n_y \end{cases} \tag{10}$$

n_x and n_y are components of the outer unit normal vector of the boundary.

In the finite element formulation, the generalized displacements and rotations can be approximated over an element by using Lagrange and Hermit interpolation functions. The second order derivatives of displacements appear in the strain-displacement relationships, implying that displacement based elements of C^1 continuity are generally necessary in the finite element procedure. Considering the fact that it is complicated to construct and implement a strict C^1 element, a four-node rectangular plate element for HSDPT is proposed here. This element has 15-DOF at each node when both bending and stretching deformations. The displacements at the element level can be defined in terms of nodal variables, as follows

$$u_0(x,y) = \sum_{i=1}^{4} u_{0i} \psi_i(x,y) + \sum_{i=1}^{4} u_{0i,x} \psi_{ix}(x,y) + \sum_{i=1}^{4} u_{0i,y} \psi_{iy}(x,y) \tag{0}$$

$$
\begin{aligned}
v_0(x,y) &= \sum_{i=1}^{4} v_{0i}\psi_i(x,y) + \sum_{i=1}^{4} v_{0i,x}\psi_{ix}(x,y) + \sum_{i=1}^{4} v_{0i,y}\psi_{iy}(x,y) \\
w_0(x,y) &= \sum_{i=1}^{4} w_{0i}\psi_i(x,y) + \sum_{i=1}^{4} w_{0i,x}\psi_i(x,y) + \sum_{i=1}^{4} w_{0i,y}\psi_i(x,y) \\
\phi_x(x,y) &= \sum_{i=1}^{4} \phi_{xi}\psi_i(x,y) + \sum_{i=1}^{4} \phi_{xi,x}\psi_{ix}(x,y) + \sum_{i=1}^{4} \phi_{xi,y}\psi_{iy}(x,y) \\
\phi_y(x,y) &= \sum_{i=1}^{4} \phi_{yi}\psi_i(x,y) + \sum_{i=1}^{4} \phi_{yi,x}\psi_{ix}(x,y) + \sum_{i=1}^{4} \phi_{yi,y}\psi_{iy}(x,y)
\end{aligned} \tag{0}
$$

where

$$
\{D_i^e\} = \{u_{0i}, v_{0i}, w_{0i}, \phi_{xi}, \phi_{yi}, u_{0i,x}, v_{0i,x}, w_{i,x}, \phi_{xi,x}, \phi_{yi,x}, u_{0i,y}, v_{0i,y}, w_{0i,y}, \phi_{xi,y}, \phi_{yi,y}\}^T \quad \text{for} \quad i = 1, 2, 3, 4. \tag{0}
$$

and the displacement interpolation functions can be written as

$$
\begin{aligned}
\psi_i &= \frac{1}{8}(1+\xi_i\xi)(1+\eta_i\eta)(2+\xi_i\xi+\eta_i\eta-\xi^2-\eta^2), \\
\psi_{ix} &= \frac{1}{8}a\xi_i(1+\xi_i\xi)^2(1+\eta_i\eta)(\xi_i\xi-1), \\
\psi_{iy} &= \frac{1}{8}b\eta_i(1+\xi_i\xi)(\eta_i\eta-1)(1+\eta_i\eta)^2,
\end{aligned} \tag{0}
$$

The normalized coordinates are defined as

$$
\xi = \frac{x-x_c}{a}, \qquad \eta = \frac{y-y_c}{b} \tag{0}
$$

where (x_c, y_c) is the center of rectangular element. a and b are the half length of plate element along *x*-axis and *y*-axis, respectively; (ξ_i, η_i) is the natural coordinates for the *i*-th node of the element.

The present element is free of the shear locking problem when the thickness of plates is small and therefore the full integration can still be used, unlike the classical Mindlin plate element (Zhang *et al*. 2013).

Eq. (8) may be expressed in the following compact form

$$
\begin{aligned}
0 = \int_0^T \Bigg\{ \int_{\Omega_0} \big[& \delta {D_0}^t (\iota_0 + z\iota_1 + z^3\iota_3)^t\, [Q](\iota_0 + z\iota_1 + z^3\iota_3) D_0 \\
& + \delta {D_0}^t (\iota_{s0} + z^2\iota_{s2})^t [Q_s](\iota_{s0} + z^2\iota_{s2}) D_0 \big] d\Omega - \int_{\Gamma_\sigma} [(\delta D_0)^t R^t F_n] dS \Bigg\} \mathrm{dt}
\end{aligned} \tag{12}
$$

where

$$R=\begin{bmatrix} n_x & n_y & 0 & 0 & \mathbf{0} \\ -n_y & n_x & \mathbf{0} & \mathbf{0} & \mathbf{0} \\ \mathbf{0} & \mathbf{0} & \mathbf{1} & \mathbf{0} & \mathbf{0} \\ \mathbf{0} & 0 & 0 & n_x & n_y \\ 0 & 0 & 0 & -n_y & n_x \end{bmatrix}, \qquad F_n=\begin{Bmatrix} \widehat{N}_n \\ \widehat{N}_{ns} \\ \widehat{Q}_n \\ \widehat{M}_n \\ \widehat{M}_{ns} \end{Bmatrix} \tag{13}$$

$$\iota_0=\begin{bmatrix} \frac{\partial}{\partial \mathrm{x}} & 0 & 0 & 0 & 0 \\ 0 & \frac{\partial}{\partial y} & 0 & 0 & 0 \\ \frac{\partial}{\partial y} & \frac{\partial}{\partial \mathrm{x}} & 0 & 0 & 0 \end{bmatrix}, \qquad \iota_1=\begin{bmatrix} 0 & 0 & 0 & \frac{\partial}{\partial \mathrm{x}} & 0 \\ 0 & 0 & 0 & 0 & \frac{\partial}{\partial y} \\ 0 & 0 & 0 & \frac{\partial}{\partial y} & \frac{\partial}{\partial \mathrm{x}} \end{bmatrix},$$

$$\iota_2=0\,, \qquad \iota_3=-c_1\begin{bmatrix} 0 & 0 & \frac{\partial^2}{\partial x^2} & \frac{\partial}{\partial \mathrm{x}} & 0 \\ 0 & 0 & \frac{\partial^2}{\partial y^2} & 0 & \frac{\partial}{\partial y} \\ 0 & 0 & 2\frac{\partial}{\partial y}\frac{\partial}{\partial \mathrm{x}} & \frac{\partial}{\partial y} & \frac{\partial}{\partial x} \end{bmatrix} \tag{14}$$

$$\iota_{s0}=\begin{bmatrix} 0 & 0 & \frac{\partial}{\partial x} & 0 & 1 \\ 0 & 0 & \frac{\partial}{\partial y} & 1 & 0 \end{bmatrix}, \qquad \iota_{s2}=-c_2\begin{bmatrix} 0 & 0 & \frac{\partial}{\partial x} & 0 & 1 \\ 0 & 0 & \frac{\partial}{\partial y} & 1 & 0 \end{bmatrix}, \qquad \iota_{s1}=0 \tag{15}$$

$$\iota_{\theta 0}=\begin{bmatrix} 1 & 0 & 0 & 0 & 0 \\ 0 & 1 & 0 & 0 & 0 \\ 0 & 0 & 1 & 0 & 0 \end{bmatrix}, \qquad \iota_{\theta 1}=\begin{bmatrix} 0 & 0 & 0 & 1 & 0 \\ 0 & 0 & 0 & 0 & 1 \\ 1 & 0 & 0 & 0 & 0 \end{bmatrix},$$

$$\iota_{\theta 2}=0 \qquad \iota_{\theta 3}=-c_1\begin{bmatrix} 0 & 0 & \frac{\partial}{\partial \mathrm{x}} & 1 & 0 \\ 0 & 0 & \frac{\partial}{\partial \mathrm{y}} & 0 & 1 \\ 0 & 0 & 0 & 0 & 0 \end{bmatrix} \tag{16}$$

Based on Eqs. (12)-(15), Eq. (16) may be expressed in the following compact form

$$\left(\delta d_0^{(e)}\right)^t \left\{ \int_{\Omega_0} \left[\sum_{i=0}^{3} {B_i}^t \left(Q_i^{(e)} B_0 + Q_{i+1}^{(e)} B_1 + Q_{i+3}^{(e)} B_3 \right) d_0^{(e)} \right. \right. \\ \left. \left. + \sum_{i=0}^{2} {B_{si}}^t \left(Q_{si}^{(e)} B_{s0} + Q_{s(i+3)}^{(e)} B_{s2} \right) d_0^{(e)} \right. \right. \tag{17}$$

$$+\sum_{i=0}^{3} {B_{\theta i}}^{t}\left(I_i^{(e)}B_{\theta 0}+I_{i+1}^{(e)}B_{\theta 1}+I_{i+3}^{(e)}B_{\theta 3}\right)d_0^{(e)}-\psi^t q^{(e)}d_0^{(e)}\Bigg]d\Omega$$
$$-\int_{\Gamma_\sigma^{(e)}}\left[\psi^t R^t F_n^{(e)}\right]dS\Bigg\}=0 \tag{17}$$

$$B_i=\iota_i\psi\,,\qquad B_{si}=\iota_{si}\psi\,,\qquad B_{\theta i}=\iota_{\theta i}\psi \tag{18}$$

$$Q_i=\int_{-h/2}^{h/2}z^i Q\,dz$$
$$Q_{si}=\int_{-h/2}^{h/2}z^i Q_s\,dz \tag{19}$$
$$I_i=\int_{-\frac{h}{2}}^{\frac{h}{2}}z^i\rho\,dz$$

$$K^{(e)}d_0^{(e)}+M^{(e)}\ddot{d}_0^{(e)}=F^{(e)} \tag{20}$$

For static analysis, the formulation of HSDPT plate can then be obtained as

$$Kd=F \tag{21}$$

And, for free vibration analysis. It can be rewritten as

$$[K-\omega^2 M]\mathrm{d}=F \tag{22}$$

where K is the global stiffness matrix, F is the global load vector, M is the global mass matrix. The above global matrices and global load vector can be obtained by assembling each corresponding element matrix and load vector, respectively. The element stiffness matrix $K^{(e)}$, element load vector $F^{(e)}$, element mass matrix $M^{(e)}$ and can be given as

$$K^{(e)}=\int_{\Omega_0}\left[\sum_{i=0}^{3}{B_i}^{t}\left(Q_i^{(e)}B_0+Q_{i+1}^{(e)}B_1+Q_{i+3}^{(e)}B_3\right)+\sum_{i=0}^{2}{B_{si}}^{t}\left(Q_{si}^{(e)}B_{s0}+Q_{s(i+3)}^{(e)}B_{s2}\right)\right]dxdy \tag{23}$$

$$M^{(e)}=\int_{\Omega_0}\left[\sum_{i=0}^{3}{B_{\theta i}}^{t}\left(I_i^{(e)}B_{\theta 0}+I_{i+1}^{(e)}B_{\theta 1}+I_{i+3}^{(e)}B_{\theta 3}\right)\right]dxdy \tag{24}$$

$$F^{(e)}=\int_{\Omega_0^{(e)}}\left(\psi^t q^{(e)}\right)+\int_{\Gamma^\sigma}\left(\psi^t R^t F_n^{(e)}\right)dS \tag{25}$$

In the present study, the Gaussian integration scheme has been implemented to evaluate integrals involved in different matrices. To prevent the shear locking phenomena, the reduced integration technique is used to integrate terms related to the transverse shear stress. In addition, natural frequencies of plate corresponding to different amplitude vibrations are obtained by analysis of the eigenvalue problem associated to Eq. (20).

4. Numerical results and discussions

In this section, firstly, the convergence and accuracy of the results is demonstrated and then the results for deflection and free vibration analyses of FG porous plates with SSSS and CCCC boundary conditions are presented. Since the results of plate made of FG porous are not available in the open literature, FG plate is used herein for the verification. For all calculations, the value of shear correction factor is taken as 5/6. The material properties of FG plates are listed in Table 1. For convenience, the following dimensionless forms are used

$$\bar{w} = \frac{E_c h^3}{q_0 a^4} w\left(\frac{a}{2}, \frac{b}{2}\right), \qquad \hat{\omega} = \omega h \sqrt{\frac{\rho_c}{E_c}}, \qquad \bar{\omega} = \omega \left(\frac{a}{h}\right)^2 \sqrt{\frac{\rho_c}{E_c}} \tag{0}$$

Table 2 shows the comparison of nondimensional deflection obtained by the present FEM with those given by Reddy (1984) based on FSDT and TSDT for different values of the thickness to length ratios (h/a = 0.05,0.1, and 0.2). It should be noted that the presented results and literature results (FSDT and TSDT) are identical especially for lower h/a ratio. It is also observed that the convergence is not depending on the thickness and the length/ thickness ration is also effected the results.

Table 3 shows the comparison of nondimensional deflections for simply supported square FG plates (h/a = 0.1) under uniform loads obtained by present FEM with those given by Zenkour (2006) based on sinusoidal shear deformation theory (SSDT) and Reddy (2000) based on the TSDT. The plates are made of a mixture of aluminum (Al) and alumina (Al2O3). In general, a good agreement between the results is obtained.

Fundamental frequency parameters of the SSSS square FG plates (a/b = 1) for different values of the thickness to length ratios (h/a = 0.05, 0.1, and 0.2) are presented in Table 4 when P = 0, 0.5, 1, 4, 10, and 1. The plates are made of a mixture of aluminum (Al) and alumina (Al2O3). It should be noted that the solutions reported by Matsunaga (2008) were based on a higher-order deformation theory, whereas Zhao *et al*. (2009) employed the FSDT by using the element-free Kp-Ritz method and Hosseini-Hashemi *et al*. (2009) obtained frequency parameters with the aid of an analytical method. In order to compare with a 3D solution, the natural frequency parameters of the SSSS

Table 1 Material properties of FG plate constituents

Properties	Aluminum(Al)	Alumina($Al_2O_{3)}$
E (GPa)	70	380
v	0.3	0.3
P (kg/m$^{3)}$	2702	3800

Table 2 Comparison of nondimensional deflection of SS plate subjected to uniformly distributed load

b/*a*	*h*/*a*	Method	$\bar{w}$
1	0.05	Present FEM	0.0444
		TSDT (Reddy 1984)	0.0444
		FSDT (Reddy 1984)	0.0444
	0.1	Present FEM	0.0466
		TSDT (Reddy 1984)	0.0467
		FSDT (Reddy 1984)	0.0467
	0.2	Present FEM	0.0534
		TSDT (Reddy 1984)	0.0535
		FSDT (Reddy 1984)	0.0536
2	0.05	Present FEM	0.1106
		TSDT (Reddy 1984)	0.1106
		FSDT (Reddy 1984)	0.1106
	0.1	Present FEM	0.1140
		TSDT (Reddy 1984)	0.1142
		FSDT (Reddy 1984)	0.1142
	0.2	Present FEM	0.1246
		TSDT (Reddy 1984)	0.1248
		FSDT (Reddy 1984)	0.1248

Table 3 Dimensionless deflection of isotropic Al/Al_2O_3 square plates under uniform loads (a/h = 10)

Method	*P*						
	0	1	2	3	5	10	metal
SSDT (Zenkour 2006)	0.04665	0.09287	0.11940	0.13200	0.14356	0.15876	2.5327
TSDT (Reddy 2000)	0.04666	0.09421	0.12227	0.13530	0.14646	0.16054	2.5328
Present FEM	0.04660	0.09389	0.12107	0.13371	0.14575	1.58941	2.5326

Table 4 Dimensionless fundamental frequency $\hat{\omega}$ of isotropic Al/Al_2O_3 square plate

h/*a*	(*m*, *n*)	Method	Power law index (*p*)				
			0	0.5	1	4	10
0.05	(1,1)	Present FEM	0.0148	0.0127	0.0112	0.0100	0.0095
		FSDT (Zhao *et al*. 2009)	0.0146	0.0124	0.0112	0.0097	0.0093
		FSDT (Hosseini-Hashemi *et al*. 2010)	0.0148	0.0128	0.0115	0.0101	0.0096
0.1	(1,1)	Present FEM	0.0578	0.0491	0.0441	0.0380	0.0363
		HSDPT (Matsunaga 2008)	0.0577	0.0492	0.0443	0.0381	0.0364
		FSDT (Zhao *et al*. 2009)	0.0568	0.0482	0.0435	0.0376	0.0359
		FSDT (Hosseini-Hashemi *et al*. 2010)	0.0577	0.0492	0.0445	0.0383	0.0363

Table 4 Continued

h/*a*	(*m*, *n*)	Method	Power law index (*p*)				
			0	0.5	1	4	10
0.1	(1,2)	Present FEM	0.1388	0.1187	0.1058	0.0897	0.0856
		HSDPT (Matsunaga 2008)	0.1381	0.1180	0.1063	0.0904	0.0859
		FSDT (Zhao *et al*. 2009)	0.1354	0.1154	0.1042	-	0.0850
	(2,2)	Present FEM	0.2130	0.1830	0.1610	0.1372	0.1295
		HSDPT (Matsunaga 2008)	0.2121	0.1819	0.1640	0.1383	0.1306
		FSDT (Zhao *et al*. 2009)	0.2063	0.1764	0.1594	-	0.1289
0.2	(1,1)	Present FEM	0.2125	0.1816	0.1638	0.1376	0.1298
		HSDPT (Matsunaga 2008)	0.2121	0.1819	0.1640	0.1383	0.1306
		FSDT (Zhao *et al*. 2009)	0.2055	0.1757	0.1587	0.1356	0.1284
		FSDT (Hosseini-Hashemi *et al*. 2009)	0.2112	0.1806	0.1650	0.1371	0.1304
	(1,2)	Present FEM	0.4672	0.4028	0.3673	0.2989	0.2771
		HSDPT (Matsunaga 2008)	0.4658	0.4040	0.3644	0.3000	0.2790
	(2,2)	Present FEM	0.6744	0.5878	0.5423	0.4350	0.3962
		HSDPT (Matsunaga 2008)	0.6753	0.5891	0.5444	0.4362	0.3981

Table 5 First three circular frequencies $\bar{\omega}$ of isotropic Al/Al_2O_3 square plate (h = 1)

a/*h*	(*m*, *n*)	Method	Power law index (*p*)		
			0	1	2
100	(1,1)	Present FEM	5.9819	4.5645	4.1610
		3D (Brischetto 2013)	5.9713	4.5529	4.1453
	(2,2)	Present FEM	23.932	18.207	16.693
		3D (Brischetto 2013)	23.860	18.195	16.564
	(3,3)	Present FEM	53.851	40.378	37.521
		3D (Brischetto 2013)	53.592	40.106	37.206
20	(1,1)	Present FEM	5.9287	4.5201	4.1237
		3D (Brischetto 2013)	5.9219	4.5193	4.1118
	(2,2)	Present FEM	23.268	17.756	16.180
		3D (Brischetto 2013)	23.108	17.681	16.054
	(3,3)	Present FEM	50.427	38.768	35.104
		3D (Brischetto 2013)	50.055	38.447	34.813
5	(1,1)	Present FEM	5.3125	4.0950	3.6979
		3D (Brischetto 2013)	5.3036	4.0923	3.6943
	(2,2)	Present FEM	16.860	13.058	11.653
		3D (Brischetto 2013)	16.882	13.278	11.876
	(3,3)	Present FEM	30.107	24.004	21.398
		3D (Brischetto 2013)	30.318	24.217	21.574

Table 6 Dimensionless Fundamental frequency of FG porous square plates (B = 0)

h/a	Boundary conditions	Coefficient of plate porosity index e_1				
		0	0.2	0.4	0.6	0.8
0.05	SSSS	0.01466	0.01417	0.01375	0.01348	0.01331
	CCCC	0.02640	0.02569	0.02497	0.02437	0.02394
0.1	SSSS	0.05729	0.05574	0.05419	0.05275	0.05193
	CCCC	0.09908	0.09635	0.09349	0.09090	0.08934
0.2	SSSS	0.21089	0.20505	0.19913	0.19357	0.19015
	CCCC	0.32871	0.31918	0.30942	0.30000	0.29364

square FG plates (a/b = 1) for different values of the length to thickness ratios (a/h = 5, 20, and 100) when P = 0, 1, 2 are presented. Keeping in mind the concept of isotropic materials as a special case of FGMs, first three circular frequencies (m = n = 1, 2, 3) as provided in Table 5, are compared with the exact elasticity solution of Brischetto (2013). From Tables 4 and 5, it can be observed that the present results are in excellent agreement with each other.

Now, we present the deflection and the natural frequencies of FG plates made of porous with CCCC, SSSS boundary conditions. Consider a square plate with the following material properties (Leclaire *et al*. 2001)

$$E_0 = 69 \text{ GPa}; \quad \rho = 2260 \frac{\text{kg}}{\text{m}^3}; \quad v = 0.25; \quad \phi = 0.3 \tag{0}$$

Table 6 lists the dimensionless fundamental frequency of the SSSS and CCCC square plates for different values of the thickness to length ratios (h/a = 0.05, 0.1, and 0.2). The coefficient of plate porosity index e_1 are selected as 0, 0.1, 0.3, 0.5. Table 7 presents the effect of Skempton

Table 7 Dimensionless Fundamental frequency of FG porous square plates (e_1 = 0)

h/a	Boundary conditions	Skempton coefficient index B			
		0.1	0.3	0.5	0.7
0.05	SSSS	0.01473	0.01495	0.01526	0.01549
	CCCC	0.0266	0.02702	0.02754	0.02784
0.1	SSSS	0.05783	0.05876	0.05954	0.06055
	CCCC	0.09965	0.10106	0.10243	0.10378
0.2	SSSS	0.21275	0.21563	0.21857	0.22162
	CCCC	0.33041	0.33373	0.33696	0.34011

Table 8 Dimensionless deflection of FG porous square plates (B = 0)

h/a	Boundary conditions	coefficient of plate porosity index e_1				
		0	0.2	0.4	0.6	0.8
0.05	SSSS	0.04618	0.05226	0.06018	0.07094	0.08637
	CCCC	0.01480	0.01675	0.01930	0.02277	0.02775

Table 8 Continued

h/*a*	Boundary conditions	coefficient of plate porosity index e_1				
		0	0.2	0.4	0.6	0.8
0.1	SSSS	0.04774	0.05405	0.06227	0.07346	0.08955
	CCCC	0.01650	0.01871	0.02159	0.02552	0.03121
0.2	SSSS	0.05398	0.06120	0.07065	0.08356	0.10221
	CCCC	0.02292	0.02606	0.03019	0.03589	0.04425

Table 9 Dimensionless deflection of FG porous square plates (e_1 = 0)

h/*a*	Boundary conditions	Skempton coefficient index B			
		0.1	0.3	0.5	0.7
0.05	SSSS	0.04543	0.04399	0.04263	0.04135
	CCCC	0.01456	0.01412	0.01369	0.01329
0.1	SSSS	0.04699	0.04555	0.04419	0.04291
	CCCC	0.01627	0.01582	0.01540	0.01500
0.2	SSSS	0.05323	0.05179	0.05043	0.04915
	CCCC	0.02269	0.02223	0.02181	0.02140

coefficient on dimensionless fundamental frequency of FG plate with various edge conditions. In Tables 8 and 9 the coefficient of plate porosity index e_1 and Skempton coefficient index B for deflection of the SSSS and CCCC square plates is studied.

In order to see better the effect coefficient of plate porosity index e_1 and Skempton coefficient index B on the natural frequencies and deflection, Figs. 2-5 also illustrate these effects for of the different plates. Figs. 2 and 4 depict the effect of coefficient of plate porosity index e_1 to the

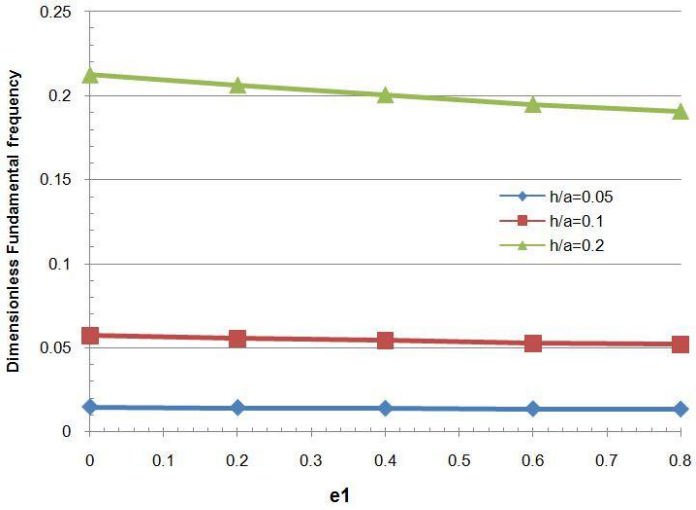

Fig. 2 Variation of Dimensionless Fundamental frequency of FG porous square plates (B = 0)

central deflection and Fundamental frequency of square FG porous plates (a/b = 1) for simply support edge with different values of the thickness to length ratios. The index e_1 indicates the effect of porosity on the solid constituents of poroelastic plate and it shows the effect of generated stresses in the pores on the poroelastic material in undrained condition (ζ = 0). Eq. (1) that the Young's modulus of elasticity depends on the porosity and it increase across the thickness direction to G_0 at top of the plate. In these figures it can be seen that the Fundamental frequency for homogeneous case is bigger than other cases and deflection for homogeneous case is less than other cases FG porous plate. It is also obvious from these figures that, by increasing the porosity in various values of thickness ratio h/a, the normalized center deflection would be increased, and Fundamental frequency decreased.

Effect of Skempton coefficient index B of the simply support square FG porous plates (a/b = 1) for different values of the thickness to length are showed in Figs. 3 and 5. Skempton pore pressure coefficient introduces the properties of the pore fluid. The values of the undrained Poisson ratio and Skempton pore pressure coefficient depend on the pore fluid compressibility. The relation between Skempton coefficient and undrained Poisson ratio for saturated case is as given by Eq. (4).

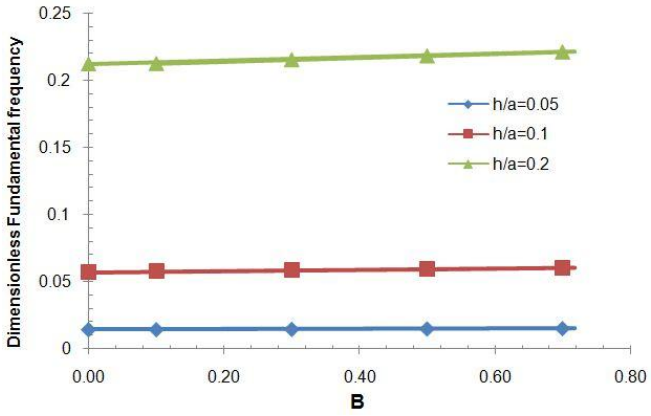

Fig. 3 Variation of Dimensionless Fundamental frequency of FG porous square plates (e_1 = 0)

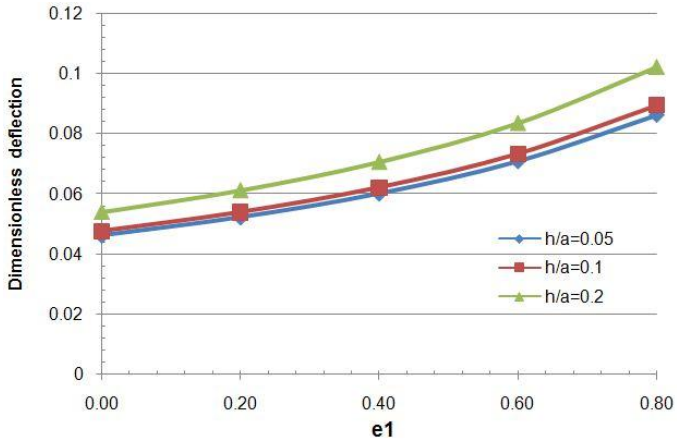

Fig. 4 Variation of dimensionless deflection of FG porous square plates (B = 0)

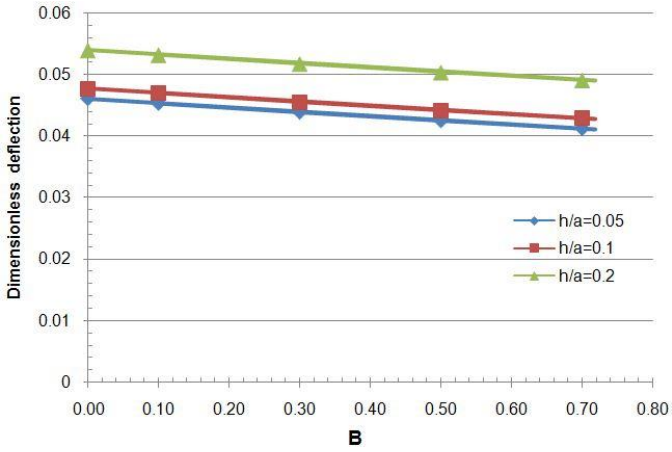

Fig. 5 Variation of dimensionless deflection of FG porous square plates ($e_1 = 0$)

If the compressibility of the pore fluid is high (B → 0), the behavior of plate resembles that of a porous plate without fluid (drained). When the compressibility of pore fluid is small (B → 1), the behavior of plate resembles that of a rigid solid. Hence, with respect to the pore fluid compressibility the Skempton coefficient changes between two values 0 and 1, (0 < B < 1). This can be observed from these figures that, by increasing the Skempton coefficient, the normalized center deflection would be decreased, and Fundamental frequency increased.

5. Conclusions

In this paper the finite element formulation based on HSDPT has been developed to analyze the deflection and free vibration in the functionally graded plates made of saturated porous material. The element proposed is a four-node rectangular element which has 15-DOF at each node with considering both bending and stretching deformations, and 9-DOF with only considering bending deformation. The present element is free of the shear locking problem when the thickness of plates is small and therefore the full integration can still be used, unlike the classical and FSDT plates' element. The boundary conditions of plate are assumed to be clamped and simply supported. Since the results of plate made of FG porous are not available in the open literature, FG plate is used herein for the verification. The numerical results obtained are in good agreement with previously published results in literature. Accuracy of the results is examined using available data in the literature. The detailed mathematical derivations and numerical investigations are presented in order to study effect of the several parameters such as porosity volume fraction, material distribution profile, mode number and boundary conditions on the natural frequencies and deflection of the PFGM plates. Finally, some new results of deflections and natural frequencies of FG porous plates are reported in tabular form for different values of Skempton coefficient and coefficient of plate porosity.

It is explicitly shown that the deflection and vibration behaviour of porous FGM plates are significantly influenced by these effects.

Based on the presented results, It is also obvious from figures that, by increasing the porosity in various values of thickness ratio *h*/*a*, the normalized center deflection would be increased, and

Fundamental frequency decreased also it is observed that from figures that, by increasing the Skempton coefficient, the normalized center deflection would be decreased, and Fundamental frequency increased. Numerical results are presented to serve as benchmarks for future analyses of FG porous structures.

References

Batra, R.C. and Jin, J. (2005), "Natural frequencies of a functionally graded anisotropic rectangular plate", *J. Sound Vib.*, **282**(1), 509-516.

Biot, M.A. (1941), "General theory of three-dimensional consolidation", *J. Appl. Phys.*, **12**(2), 155-164.

Biot, M.A. (1955), "Theory of elasticity and consolidation for a porous anisotropic solid", *J. Appl. Phys.*, **26**(2), 182-185.

Biot, M.A. (1964), "Theory of buckling of a porous slab and its thermoelastic analogy", *J. Appl. Mech.*, **31**(2), 194-198.

Biot, M.A. (1956), "Theory of propagation of elastic waves in a fluid-saturated porous solid. Parts I and II", *J. Acoust. Soc. Am.*, **28**(2), 168-191.

Biot, M.A. and Willis, D.G. (1957), "The elastic coefficients of the Theory of Consolidation", *J. Appl. Mech.*, **24**, 594-601.

Brischetto, S. (2013), "Exact elasticity solution for natural frequencies of functionally graded simply-supported structures", *Comput. Model. Eng. Sci.*, **95**(5), 391-430.

Carrera, E. and Brischetto, S. (2008), "Analysis of thickness locking in classical, refined and mixed multilayered plate theories", *Compos. Struct.*, **82**(4), 549-562.

Civalek, O. (2008), "Free vibration analysis of symmetrically laminated composite plates with first-order shear deformation theory (FSDT) by discrete singular convolution method", *Finite Elem. Anal. Des.*, **44**(12-13), 725-731.

Civalek, O. (2009), "Fundamental frequency of isotropic and orthotropic rectangular plates with linearly varying thickness by discrete singular convolution method", *Appl. Math. Model.*, **33**(10), 3825-3835.

Civalek, O. (2013), "Vibration analysis of laminated composite conical shells by the method of discrete singular convolution based on the shear deformation theory", *Compos. Part-B: Eng.*, **45**(1), 1001-1009.

Ebrahimi, F. and Mokhtari, M. (2014), "Transverse vibration analysis of rotating porous beam with functionally graded microstructure using the differential transform method", *J. Brazil. Soc. Mech. Sci. Eng.*, **37**(4), 1-10.

Ebrahimi, F. (2013), "Analytical investigation on vibrations and dynamic response of functionally graded plate integrated with piezoelectric layers in thermal environment", *Mech. Adv. Mater. Struct.*, **20**(10), 854-870.

Ebrahimi, F. and Rastgoo, A. (2008a), "Free vibration analysis of smart annular FGM plates integrated with piezoelectric layers", *Smart Mater. Struct.*, **17**(1), 015044.

Ebrahimi, F. and Rastgoo, A. (2008b), "An analytical study on the free vibration of smart circular thin FGM plate based on classical plate theory", *Thin-Wall. Struct.*, **46**(12), 1402-1408.

Ebrahimi, F., Rastgoo, A. and Atai, A.A. (2009a), "A theoretical analysis of smart moderately thick shear deformable annular functionally graded plate", *Eur. J. Mech.-A/Solids*, **28**(5), 962-973.

Ebrahimi, F., Naei, M.H. and Rastgoo, A. (2009b), "Geometrically nonlinear vibration analysis of piezoelectrically actuated FGM plate with an initial large deformation", *J. Mech. Sci. Technol.*, **23**(8), 2107-2124.

Ebrahimi, F. and Rastgoo, A. (2011), "Nonlinear vibration analysis of piezo-thermo-electrically actuated functionally graded circular plates", *Arch. Appl. Mech.*, **81**(3), 361-383.

Fatt, I. (1959), "The Biot-Willis elastic coefficients for a sandstone", *J. Appl. Mech.*, **26**(28), 296-297.

Ferreira, A.J.M., Batra, R.C., Roque, C.M.C., Qian, L.F. and Jorge, R.M.N. (2006), "Natural frequencies of functionally graded plates by a meshless method", *Compos. Struct.*, **75**(1), 593-600.

Ghassemi, A. and Zhang, Q. (2004), "A transient fictitious stress boundary element method for porothermoelastic media", *Eng. Anal. Bound. Elem.*, **28**(11), 1363-1373.
Hashin, Z. and Shtrikman, S. (1963), "A variational approach to the theory of the elastic behaviour of multiphase materials", *J. Mech. Phys. Solid.*, **11**(2), 127-140.
Hosseini-Hashemi, S., Taher, H.R.D., Akhavan, H. and Omidi, M. (2010), "Free vibration of functionally graded rectangular plates using first-order shear deformation plate theory", *Appl. Math. Model.*, **34**(5), 1276-1291.
Jabbari, M., Mojahedin, A., Khorshidvand, A.R. and Eslami, M.R. (2013a), "Buckling analysis of a functionally graded thin circular plate made of saturated porous materials", *J. Eng. Mech.*, **140**(2), 287-295.
Jabbari, M., Joubaneh, E.F., Khorshidvand, A.R. and Eslami, M.R. (2013b), "Buckling analysis of porous circular plate with piezoelectric actuator layers under uniform radial compression", *Int. J. Mech. Sci.*, **70**, 50-56.
Jabbari, M., Hashemitaheri, M., Mojahedin, A. and Eslami, M.R. (2014a), "Thermal buckling analysis of functionally graded thin circular plate made of saturated porous materials", *J. Therm. Stress.*, **37**(2), 202-220.
Jabbari, M., Joubaneh, E.F. and Mojahedin, A. (2014b), "Thermal buckling analysis of porous circular plate with piezoelectric actuators based on first order shear deformation theory", *Int. J. Mech. Sci.*, **83**, 57-64.
Khorshidvand, A.R., Joubaneh, E.F., Jabbari, M. and Eslami, M.R. (2014), "Buckling analysis of a porous circular plate with piezoelectric sensor–actuator layers under uniform radial compression", *Acta Mechanica*, **225**(1), 179-193.
Leclaire, P., Horoshenkov, K.V. and Cummings, A. (2001), "Transverse vibrations of a thin rectangular porous plate saturated by a fluid", *J. Sound Vib.*, **247**(1), 1-18.
Magnucka-Blandzi, E. (2008), "Axi-symmetrical deflection and buckling of circular porous-cellular plate", *Thin-Wall. Struct.*, **46**(3), 333-337.
Matsunaga, H. (2008), "Free vibration and stability of functionally graded plates according to a 2-D higher-order deformation theory", *Compos. Struct.*, **82**(4), 499-512.
Ng, C.H.W., Zhao, Y.B. and Wei, G.W. (2004), "Comparison of discrete singular convolution and generalized differential quadrature for the vibration analysis of rectangular plates", *Comput. Method. Appl. Mech. Eng.*, **193**(23-26), 2483-2506.
Reddy, J.N. (1984), "A refined nonlinear theory of plates with transverse shear deformation", *Int. J. Solid. Struct.*, **20**(9), 881-896.
Reddy, J.N. (1993), *An Introduction to the Finite Element Method*, (Vol. 2, No. 2.2), McGraw-Hill, New York, NY, USA.
Reddy, J.N. (2000), "Analysis of functionally graded plates", *Int. J. Numer. Method. Eng.*, **47**(1-3), 663-684.
Reddy, J.N. (2004), *Mechanics of Laminated Composite Plates and Shells*: *Theory and Analysis*, CRC press.
Reddy, J.N. and Cheng, Z.Q. (2003), "Frequency of functionally graded plates with three-dimensional asymptotic approach", *J. Eng. Mech.*, **129**(8), 896-900.
Thai, H.T. and Choi, D.H. (2014), "Finite element formulation of a refined plate theory for laminated composite plates", *J. Compos. Mater.*, **48**(28), 3521-3538.
Theodorakopoulos, D.D. and Beskos, D.E. (1994), "Flexural vibrations of poroelastic plates", *Acta Mech.*, **103**(1-4), 191-203.
Vel, S.S. and Batra, R.C. (2004), "Three-dimensional exact solution for the vibration of functionally graded rectangular plates", *J. Sound Vib.*, **272**(3), 703-730.
Wattanasakulpong, N. and Chaikittiratana, A. (2015), "Flexural vibration of imperfect functionally graded beams based on Timoshenko beam theory: Chebyshev collocation method", *Meccanica*, **50**(5), 1-12.
Zenkour, A.M. (2006), "Generalized shear deformation theory for bending analysis of functionally graded plates", *Appl. Math. Model.*, **30**(1), 67-84.
Zenkour, A.M. (2009), "The refined sinusoidal theory for FGM plates on elastic foundations", *Int. J. Mech. Sci.*, **51**(11), 869-880.
Zhang, B., He, Y., Liu, D., Gan, Z. and Shen, L. (2013), "A non-classical Mindlin plate finite element based

on a modified couple stress theory", *Eur. J. Mech. - A/Solids*, **42**, 63-80.
Zhao, X., Lee, Y.Y. and Liew, K.M. (2009), "Free vibration analysis of functionally graded plates using the element-free kp-Ritz method", *J. Sound Vib.*, **319**(3), 918-939.

CC